

Enhancing Consistency and Mitigating Bias: A Data Replay Approach for Incremental Learning

Chenyang Wang, Junjun Jiang, *Senior Member, IEEE*, Xingyu Hu, Xianming Liu, *Member, IEEE*,
Xiangyang Ji, *Senior Member, IEEE*

Abstract—Deep learning systems are prone to catastrophic forgetting when learning from a sequence of tasks, where old data from experienced tasks is unavailable when learning from a new task. To mitigate the problem, a line of methods propose to replay the data of experienced tasks when learning new tasks. These methods usually adopt an extra memory to store the data for replay. However, it is not expected in practice considering the memory constraint or data privacy issue. As a replacement, data-free data replay methods are proposed by inverting samples from the classification model. Though achieving good results, these methods still suffer from the inconsistency of the inverted and real training data, which is neglected in the inversion stage in recent works. To that effect, we propose to measure the data consistency quantitatively by some simplification and assumptions. Using the measurement, we analyze existing techniques for inverting samples and get some insightful information that inspires a novel loss function to reduce the inconsistency. Specifically, the loss minimizes the KL divergence of the distributions of inverted and real data under the tied multivariate Gaussian assumption, which is easy to implement in continual learning. In addition, we observe that the norms of old class weights turn to decrease continually as learning progresses. We thus analyze the underlying reasons and propose a simple regularization term to balance the class weights so that the samples of old classes are more distinguishable. To conclude, we propose the Consistency enhanced data replay with debiased classifier for Class Incremental Learning (CCIL). Extensive experiments on CIFAR-100, Tiny-ImageNet, and ImageNet100 show consistently improved performance of CCIL compared to previous approaches.

Index Terms—Incremental learning, Data replay, Data consistency, Classifier Bias.

I. INTRODUCTION

THE common practice of training a deep model in the computer vision community is to collect a big enough dataset first and then train offline based on the collected dataset [1]–[3]. However, this kind of training scheme has some limitations. For example, during deployment, when unexpected events occur or new tasks appear, the model needs retraining on both the old and the newly encountered data, which is costly. What is more, data storage is always limited in practice and can not save all the data when tasks continually come. In addition, saving the encountered data permanently may incur privacy issues [4]. Taking these problems into account, a model that can learn from a sequence of tasks is in

C. Wang, J. Jiang, X. Hu and X. Liu are with the School of Computer Science and Technology, Harbin Institute of Technology, Harbin 150001, China. E-mail: {cswcy, jiangjunjun, huxingyu, csxm}@hit.edu.cn.

X. Ji is with the Department of Automation, Tsinghua University, Beijing 100084, China. E-mail: xyji@tsinghua.edu.cn.

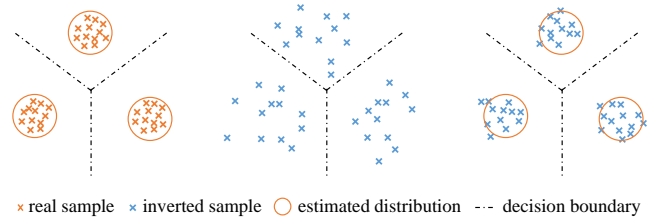


Fig. 1. Schematic illustration of data consistency enhancement. Left, the situation of real samples. The distribution is estimated from real samples. Middle, the situation of inverted samples before data consistency enhancement. Right, the situation of inverted samples after consistency enhancement.

need. However, when training data changes, the knowledge learned before in the deep models will be catastrophically forgotten [5]. In this paper, we mainly focus on the class incremental learning (CIL) setting, where data in different tasks are belonging to different classes and the purpose is to classify samples from all classes without the task information.

To avoid catastrophic forgetting, some researchers proposed revising the old knowledge by replaying the data of experienced tasks when learning the new task. Some works achieved this goal by keeping an extra data memory with a fixed size and designing specific strategies to manage and learn from the limited data in the memory [6]–[8]. Different from them, other methods tried to incrementally train a generator to generate old samples [9]–[11] and learn from the generated data, which is not constrained by the number of samples but by the generation quality. What is more, they still needed memory for saving the generator in the whole incremental learning process. Regarding memory constraints and latent privacy issues in practice, both the two lines of methods are not that applicable.

To fulfill these visions, there are some works [12], [13] that aim at performing class incremental learning in a data-free manner, called data-free class incremental learning (DFCIL). That is, neither extra data memory nor an extra generation model is available in the data replay stage. These works mainly build upon the idea of inversion-based data-free knowledge distillation [14]–[16] by inverting samples directly from the classification model. It is natural to introduce the technique into data-free CIL, where at each new learning phase, the trained model on experienced tasks is available but the previous data is inaccessible. As for these data replay-based methods, the memory constraint problem and latent privacy issues are sidestepped properly. But they still face the inversion quality problem, which is severe for the lack of data. Thus,

existing methods made great efforts on how to distill from these inverted samples and achieve SOTA performance.

Despite their success, the inversion quality problem further incurs data inconsistency between synthetic and real samples, which is left unsolved and ignored by existing methods. Different from them, we focus on the inversion stage and consider how to narrow the distribution gap, which is orthogonal to previous works. The schematic illustration of our motivation can be found in Figure 1. We argue that the efforts in the inversion stage will help the overall performance. Because in the ideal case, the distribution of synthetic data is the same as the real data and the CIL problem degenerates into an offline supervised learning problem, which is much easier to solve. To that effect, we propose two metrics to quantitatively measure the data consistency by some simplification and assumptions. With them, we take a closer look at the existing techniques and find that there is still room to further improve data consistency. It inspires a new loss term. Specifically, we model the data distribution in the representation space of the penultimate layer and align the estimated distributions of old real and synthetic samples accordingly. It is natural to implement in the incremental learning setting: we estimate the parameters of the distributions at the end of the old task and when the new task comes, we regularize the synthetic samples to have similar statistics as the estimated ones to enhance consistency.

On the other hand, we observe an unexpected phenomenon during incremental learning, where the norm of weight vectors belonging to old classes is lower than that belonging to new classes. It is similar to the observation in [17], but the underlying reasons are different. In [17], the class imbalance between replay data and new data is contributed to the biased class vectors. However, in inversion-based methods, the different learning strategies and different properties of synthetic data and real data take the major responsibility. Unlike [17] where a post-processing refinement of class vectors is introduced, we propose to add a regularization term to align the unbiased class weights. In this way, the network and weight vectors are optimized together in an unbiased and matching manner, which is more friendly to the inversion stage.

The main contributions of this work are summarized as follows:

- We measure the data consistency of synthetic and real old data with some simplification. Using the measurement, we analyze existing inversion losses and draw insightful information, which inspires us to enhance the data consistency with a novel loss term.
- We analyze the underlying reasons for the biased class vectors when learning from both synthetic data and new data and put forward a simple regularization term that is friendly to the inversion stage.
- Through extensive experiments on different datasets, we show that our method can be combined with different baselines and achieve SOTA performance.

The rest of the paper is unfolded as follows. Section II introduces related works of our method, including works for class incremental learning and consistency measurement. Section IV introduces the preliminaries of our work, presents the overall framework, and depicts consistency enhanced replay and the

debiased classifier, and Section V shows the comparison results of our proposed method with others, ablation study, and parameter analysis. Section VI concludes this study.

II. RELATED WORK

A. Class Incremental Learning

There is a rich literature in class incremental learning and methods of different categories try to solve the catastrophic forgetting problem of CIL from different views. Some works [18]–[23] propose to incrementally expand the network to adapt to classes of different tasks and the modules can perform as a whole to classify all the seen classes during the testing stage. One other effective strategy to alleviate catastrophic forgetting is to regularize the optimization of the deep model when learning new tasks. Lots of works [24]–[27] in this line are proposed based on different understandings of how to maintain the important information of past tasks. What is more, some research improves the performance of CIL with the help of other extra resources like extra unlabeled data [28], [29], pretrained models [20], or prompts [30].

Methods [6], [7], [31]–[34] mostly related to ours are based on knowledge distillation [35], where data representing past tasks are available to replay. To name some, iCaRL [6] performed logits distillation between the old model and the new model on both the data stored in the memory and data of the new task, UCIR [33] proposed to distill the features between the old model and the new model, PODNet [7] alternatively chose to distill the pooled feature maps in multiple layers, and INP-LPP [34] preserved both the global property of the whole set and the ranking of the label with instance neighborhood-preserving loss and label priority-preserving loss during distillation. Instead of storing data in memory, some works [10] additionally keep a generative model in memory to generate enough samples for distillation. Despite their effectiveness and popularity, all these methods need a relatively big memory budget to perform well.

B. Data-free Replay-based Class Incremental Learning

Data-free class incremental learning refers to CIL without storing either generative models or training data from past tasks. To tackle this, LwF [36] substituted data in the new task for old encountered data for distillation. Owing to the distribution difference between new task data and old task data, the performance of LwF is relatively limited. On top of that, [37] proposed to only perform distillation on a subset of new data samples selected by normalized cosine scores between samples and saved prototypes. To close the gap between data for distillation and data encountered, [14] inverted the data for distillation from the classification model independently. However, this method failed when applied to the standard benchmark of class incremental learning. The underlying reason is the gap between the synthetic samples and real samples. To facilitate the learning, [12] designed the modified cross-entropy training and importance-weighted feature distillation. The following work [13] split the representation learning stage and classification refinement stage. During representation learning, [13] adopted a relation-guided distillation loss to

alleviate the conflict between plasticity and stability. What is more, [38] built upon the inversion stage proposed in [15] and proposed an additional strategy to guarantee the quality of inverted samples by virtue of the memorized confusion matrix.

C. Data Consistency Measurement

GAN [39] loss is a widely-used and effective loss to generate samples that are indistinguishable from target samples. However, it is not suitable in our setting where no target data is available. Domain alignment methods [40]–[42] in domain generalization are also related to the measurement of data consistency. But unlike generating consistent data in our setting, domain alignment methods align data of different domains in the feature space with the help of additional models and/or data. The setting most relative to our work is the inference-time OOD detection [43]–[46], where a pretrained classification model is frozen and training data is accessible (just like the end of the task in incremental learning). Our work builds on the assumptions proposed in [43] and proposes to align the statistical parameters in the feature space to enhance data consistency.

III. PRELIMINARIES

A. Problem Settings

The purpose of class incremental learning is to learn a model that can tell the classes of all encountered training samples that come as a sequence of tasks. We formulate it as follows. Suppose $\mathcal{T}_0, \mathcal{T}_1, \dots, \mathcal{T}_{N-1}$ are the N tasks to be learned sequentially. The label set \mathcal{C}_i of \mathcal{T}_i meets the following condition: $\forall i, j, i \neq j, \mathcal{C}_i \cap \mathcal{C}_j = \emptyset$, which indicates that two samples from different tasks can not belong to the same class. After learning $\mathcal{T}_0, \mathcal{T}_1, \dots, \mathcal{T}_{N-1}$ (denoted as $\mathcal{T}_{0:N-1}$), the classification model is supposed to classify samples from all seen classes $\mathcal{C}_0 \cup \mathcal{C}_1 \cup \dots \cup \mathcal{C}_{N-1}$ (denoted as $\mathcal{C}_{0:N-1}$). On top of that, at task \mathcal{T}_i in our setting, samples belonging to classes in \mathcal{C}_i are sufficient while no samples belonging to past tasks $\mathcal{T}_{0:i-1}$ are accessible. The classification model to be trained is denoted as $f(\cdot)$ which is composed of a feature extractor $h(\cdot)$ which has the deep neural network architecture, and a classifier $g(\cdot)$ which is the final fully-connected layer, that meets: $f(\cdot) = g(h(\cdot))$.

B. Baseline Approach

In this section, we introduce a baseline method. For the inversion stage, the objective is to invert input samples from a classification model. To that effect, we froze the model and optimize the pixels of inputs according to some losses on the features and outputs. We adopt DeepInversion [14] in this baseline just like other SOTA DFCIL methods [12], [13].

The first component is the cross-entropy loss based on the assumption that inverted samples can be classified correctly by the old model. Let us denote the inverted samples at \mathcal{T}_i as \hat{X}^{i-1} , the old model as $f_{0:i-1}$. The cross-entropy loss is given as follows:

$$\mathcal{L}_{ce} = \frac{1}{|\hat{X}^{i-1}|} \sum_{(\hat{x}, \hat{y}) \in \hat{X}^{i-1}} \ell_{ce}(f_{0:i-1}(\hat{x}), \hat{y}, \tau), \quad (1)$$

where τ is the temperature.

Besides, the statistics alignment loss is proposed to align the Batch Normalization (BN) statistics. Each BN layer stores the running mean and variance of features, which can be directly utilized as the prior knowledge to regularize the inversion stage as follows:

$$\mathcal{L}_{stat} = \sum_l \mathcal{D}_{KL}(\mathcal{N}(\sigma_l, \mu_l), \mathcal{N}(\hat{\sigma}_l, \hat{\mu}_l)), \quad (2)$$

where l indicates the l -th BN layer in the model, σ_l, μ_l denotes the mean and variance of the i -th BN layer stored in the old model, $\hat{\sigma}_l, \hat{\mu}_l$ denotes the mean and variance estimated on the inverted data, and \mathcal{D}_{KL} denotes the KL divergence.

Following [12], [13], to improve the efficiency of the inversion, a generator $G(\cdot)$ with trainable parameters is introduced to generate input samples: $\hat{x} = G(n), \hat{y} = \arg\max_k f_{0:i-1}(\hat{x})_k$, where n is the noise. By introducing the generator, parameters to be optimized change from pixels of inputs \hat{X}^{i-1} to parameters of $G(\cdot)$. To guarantee class balance in the generated data, a class diversity loss is adopted in the baseline as follows:

$$\mathcal{L}_{div} = H \left(\frac{1}{|\hat{X}^{i-1}|} \sum_{(\hat{x}, \hat{y}) \in \hat{X}^{i-1}} \text{Softmax}(f_{0:i-1}(\hat{x})) \right), \quad (3)$$

where H denotes the information entropy. We remark that the generator is not necessary for the inversion stage and one can directly optimize \hat{X}^{i-1} with a sacrifice to the inversion efficiency. Also, note that, unlike generative data replay [10], the generator here is inverted only from $f_{0:i-1}$ and can be immediately discarded after data inversion, which is viewed as data-free in CIL.

The overall loss for the inversion stage is:

$$\mathcal{L}_{I_base} = \mathcal{L}_{ce} + \lambda_1 \mathcal{L}_{stat} + \lambda_2 \mathcal{L}_{div}, \quad (4)$$

where λ_1, λ_2 are hyperparameters controlling the scales of the losses.

As for the training stage, we adopt R-DFCIL [13] as our baseline because of its SOTA performance. In R-DFCIL, hard knowledge distillation (HKD) is proposed to distill the information of old tasks, local cross-entropy loss (LCE) is adopted for learning from samples of current tasks, and relational knowledge distillation loss builds a bridge for old and new models when training with new samples. We denote the baseline training loss as \mathcal{L}_{T_base} . To be noticed, our method is orthogonal to previous works contributing to the distillation losses and can be combined with any of them (See details in Section V-B).

The details of HKD and LCE are provided here for the latter analysis. HKD is applied on synthetic samples to prevent model changes as follows:

$$\mathcal{L}_{hkd} = \frac{1}{|\hat{X}^{i-1}| \times |\mathcal{C}_{0:i-1}|} \sum_{(\hat{x}, \hat{y}) \in \hat{X}^{i-1}} \|f_{0:i-1}(\hat{x}) - f_{0:i}(\hat{x})\|_1. \quad (5)$$

Then, a cross-entropy loss is applied locally to the current task's samples (denoted as X^i) as follows:

$$\mathcal{L}_{lce} = \frac{1}{|X^i|} \sum_{(x, y) \in X^i} \ell_{ce}(f_i(x), y, \tau), \quad (6)$$

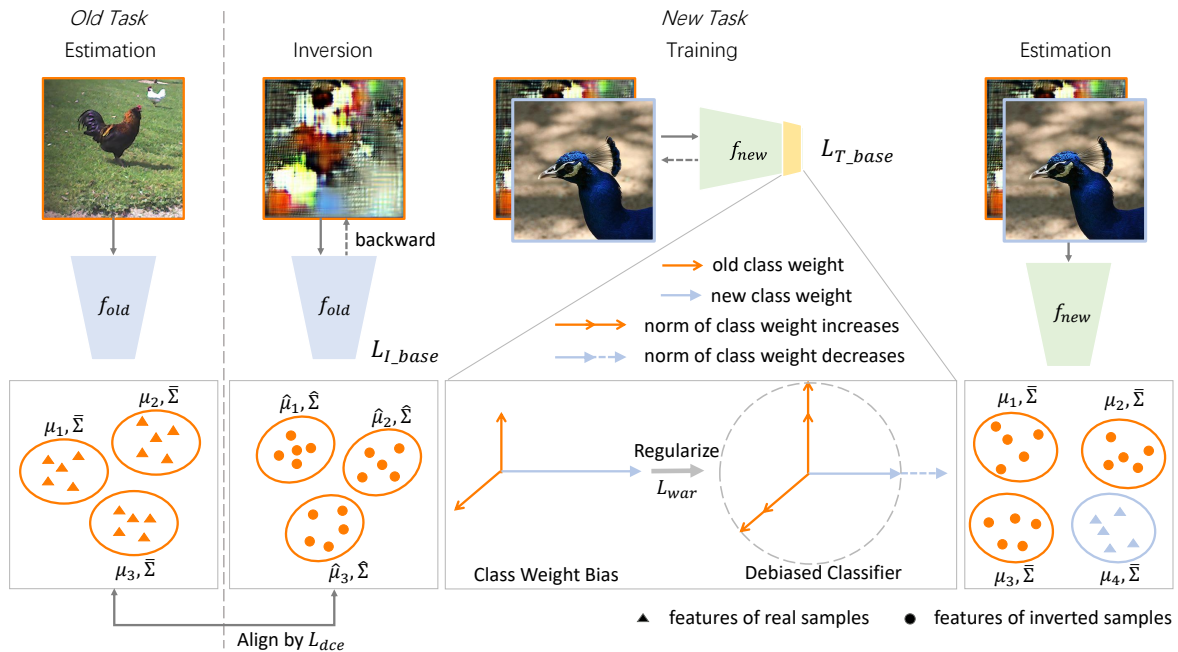


Fig. 2. An overview of our proposed CCIL framework. Inversion: when a new task comes, we first invert samples from the old model with the help of statistical parameters in the old task. Data consistency enhancement loss L_{dce} is applied in this stage. Training: we use the inverted data and real new data to train a new model. During the training stage, we regularize the class weights to be unbiased by weight alignment regularization loss L_{war} . Estimation: when training is over, we estimate the statistical parameters of all classes by the new model.

where $f_i(\cdot) = g_i(h_{0:i}(\cdot))$, that apply Softmax on the logits of classes belonging to the current task.

IV. METHOD

A. Overall Framework

The challenge of the incremental learning setting is how to preserve the knowledge of past tasks when past data are inaccessible. To cope with it, we propose the Consistency enhanced data replay with debiased classifier for Class Incremental Learning (CCIL). CCIL framework consists of three stages within each task. (1) Inversion. The purpose of the inversion stage is to synthesize samples as a substitute for past data. In this stage, we regularize the statistics of synthetic samples to be the same as the past samples with the help of the old model and the statistical parameters from the last task. Our data consistency enhancement (DCE) loss is applied in this stage. (2) Training. In the training stage, a new model inherited from the old model is trained to classify data from all tasks. During the training stage, we propose a weight alignment regularization (WAR) loss to debias the class weights. (3) Estimation. When training is finished, statistical parameters characterizing classes of all encountered tasks will be estimated and memorized for the following task. To be noticed, for the first task, only training and estimation stages are in need and only real samples are involved in the training stage. The overall framework can be found in Figure 2.

B. Consistency Enhanced Data Replay

1) **Estimate Data Consistency:** Our goal is to enhance the consistency between the real and synthetically replayed samples in the inversion stage to facilitate the following

TABLE I
EFFECTS OF DIFFERENT LOSSES ON DATA CONSISTENCY. WE ABLATE LOSS COMPONENTS OF THE BASELINE LOSS AND SHOW THE IMPROVEMENT AFTER COMBINING L_{dce} .

Method	$D_{KL}(KDE)$	$D_{KL}(Gaussian)$
$L_{ce}+L_{div}$	42.6510	253.9446
$L_{stat}+L_{div}$	33.2941	21.0037
$L_{ce}+L_{stat}+L_{div}$	32.5018	22.5027
$L_{ce}+L_{stat}+L_{div}+L_{dce}$	30.4094	16.4198

training stage of the new task. To begin with, we try to measure the consistency quantitatively. Denote the probability of real samples as $p(x)$ and synthetic samples as $q(x)$, it is natural to measure the consistency of the two distributions by the KL divergence: $D_{KL} = \mathbb{E}_p \log \frac{p(x)}{q(x)}$. However, directly computing D_{KL} is infeasible in practice due to the high dimension of the image space. What is more, the metrics about pixel differences lack sufficient semantic interpretation. Instead, we pay attention to the output features of the penultimate layer (i.e., $z = h(x)$), the input of the classifier $g(\cdot)$, because it has a relatively low dimension and directly and evidently affects the final classification performance as also discussed in the literature of CIL [47], [48] and more [44], [49].

To estimate $p(z)$ and $q(z)$, we adopt the kernel density estimation (KDE) technique. Specifically, we use the Gaussian kernel and decide the bandwidth by Scott's method [50]. With estimated $p(z)$ and $q(z)$, one can calculate D_{KL} . But owing to no analytical solution and high computational complexity, we approximate KL divergence with Monte-Carlo approximation¹. Though performing estimation in this way is feasible

¹We follow the algorithm in <http://joschu.net/blog/kl-approx.html>.

and the estimated KL divergence can be used as a metric, it is inefficient in computing and is not differential to the inverted samples in the inversion stage which incurs difficulties when adopting it as the objective function.

To fulfill the vision of efficiency and differentiability, we further assume that the class-conditional distribution in the feature space follows a tied multivariate Gaussian distribution. It is reasonable for the theoretical connection between Gaussian discriminant analysis and the SoftMax classifier and the empirical results detailed in [43]. To be specific, given any class k , denote the feature set of class k as Z_k satisfying: $Z_k \sim \mathcal{N}(\mathbf{u}_k, \bar{\Sigma})$, where \mathbf{u}_k is the mean vector and $\bar{\Sigma}$ is the tied covariance matrix. The parameters can be estimated easily: $\mathbf{u}_k = \frac{1}{|Z_k|} \sum_{z \in Z_k} z$, $\bar{\Sigma} = \frac{1}{|Z|} \left(\sum_k \sum_{z \in Z_k} (z - \mathbf{u}_k)(z - \mathbf{u}_k)^T \right)$, where $Z = \bigcup_k Z_k$. In addition, $p(k)$ can be estimated by $|Z_k|/|Z|$. $p(z)$ is then given as follows:

$$p(z) = \sum_k p(k) \mathcal{N}(z | \mathbf{u}_k, \bar{\Sigma}). \quad (7)$$

$q(z)$ can be estimated similarly in spite that \hat{Z} is the feature set of synthetic samples. Because there is no analytical form of D_{KL} between the mixtures of Gaussians, we adopt the Monte-Carlo approximation method as above.

2) **Analysis of Existing Losses:** With the two KL Divergence metrics, we try to study the effects of losses proposed in the literature under a unified framework. We first train a model with 50 classes in CIFAR-100 and then invert samples from it. Then, the KL divergences of inverted and real old data approximated in two ways are given. We ablate the loss components of the inversion baseline and the results can be found in Table I.

We can draw some conclusions from Table I. First, the results of D_{KL} (KDE) and D_{KL} (Gaussian) are similar, which corroborate each other and can reflect the relative data consistency among methods. Second, the cross-entropy loss does not contribute to data consistency much. It is intuitive because cross-entropy loss is a sample-wise measurement and lacks any direct constraint on either the diversity or the distribution. What is more, minimizing the cross-entropy loss in Equation (1) equals maximizing the Softmax score of samples. But it is well-studied that Softmax score [51] is not a good metric for OOD detection [44], [45] and thus for data consistency measurement. Note in our experiments, the cross-entropy is not indispensable. We keep it for it does not contradict other losses during training and can slightly improve the performance in some cases. Third, the statistics alignment loss indeed ameliorates the consistency, but there is still plenty of room. We observe that the alignment in Equation (2) only considers the features of the BN layers but lacks explicit regularization on non-BN layer features, such as features of the important penultimate layer. To that effect, we propose the data consistency enhancement loss L_{dce} on the features of the penultimate layer described below. Combining L_{dce} , the data consistency is further enhanced as desired.

3) **Data Consistency Enhancement Loss:** In what follows, we give the details of L_{dce} , which intends to align the distributions of real and synthetic data under the aforementioned

Multivariate Gaussian assumption. Formally, given any class $k \in \mathcal{C}_{0:N-1}$ and its data X_k , denote the feature vectors of X_k as $h(X_k)$ and $h(X_k)$ satisfies: $h(X_k) \sim \mathcal{N}(\mathbf{u}_k, \bar{\Sigma})$. In the incremental learning setting, we estimate $\mathbf{u}_0, \mathbf{u}_1, \dots, \mathbf{u}_{|\mathcal{C}_{0:i}|}$ and $\bar{\Sigma}$ at the end of each task \mathcal{T}_i with $h_{0:i}(\cdot)$ as follows:

$$\mathbf{u}_k = \begin{cases} \frac{1}{|\hat{X}_k^{i-1}|} \sum_{\hat{x} \in \hat{X}_k^{i-1}} h_{0:i}(\hat{x}), & \text{if } k \notin \mathcal{C}_i, \\ \frac{1}{|X_k|} \sum_{x \in X_k} h_{0:i}(x), & \text{if } k \in \mathcal{C}_i, \end{cases} \quad (8)$$

$$\bar{\Sigma} = \frac{1}{|\hat{X}^{i-1} \cup X^i|} \left(\sum_{k \notin \mathcal{C}_i} \sum_{\hat{x} \in \hat{X}_k^{i-1}} (h_{0:i}(\hat{x}) - \mathbf{u}_k)(h_{0:i}(\hat{x}) - \mathbf{u}_k)^T + \sum_{k \in \mathcal{C}_i} \sum_{x \in X_k} (h_{0:i}(x) - \mathbf{u}_k)(h_{0:i}(x) - \mathbf{u}_k)^T \right), \quad (9)$$

where \hat{X}^{i-1} denotes the data inverted from $f_{0:i-1}$ and \hat{X}_k^{i-1} denotes the inverted data of class k . Then, to align the synthetic data \hat{X}^i in task \mathcal{T}_{i+1} and data $\hat{X}^{i-1} \cup X^i$ in task \mathcal{T}_i , we estimate corresponding parameters of \hat{X}^i as follows:

$$\hat{\mathbf{u}}_k = \frac{1}{|B_k|} \sum_{\hat{x} \in \hat{X}_k^i \cap B} h_{0:i}(\hat{x}) \quad (10)$$

$$\hat{\Sigma} = \frac{1}{|B|} \sum_k \sum_{\hat{x} \in \hat{X}_k^i \cap B} (h_{0:i}(\hat{x}) - \hat{\mathbf{u}}_k)(h_{0:i}(\hat{x}) - \hat{\mathbf{u}}_k)^T, \quad (11)$$

where $|B_k|$ is the number of inverted samples belonging to class k in batch B and $|B|$ is the batch size. To enhance the consistency between inverted and real data, we directly align the parameters as follows:

$$\mathcal{L}_{dce} = \sum_k \|\hat{\mathbf{u}}_k - \mathbf{u}_k\|_2 + \|\hat{\Sigma} - \bar{\Sigma}\|_F. \quad (12)$$

In ideal situation, we guarantee $p(z|k) = q(z|k)$ by Equation (12) and $p(k) = q(k)$ by Equation (3). Thus, we align $p(z)$ and $q(z)$. The overall loss for our consistency-enhanced data replay training is:

$$\mathcal{L}_{inv} = \mathcal{L}_{I_base} + \lambda_{dce} \mathcal{L}_{dce}. \quad (13)$$

The proposed DCE loss can be naturally implemented in the context of the DFCIL setting. Specifically, it is viable to estimate the old class distributions with all training samples at the end of the task. And the estimated statistical parameters can be combined with the old model seamlessly to enhance the data consistency in the inversion stage of the new task.

C. Debiased Classifier

By treating real and synthetic samples differently, the works of [12], [13] successfully circumvented the domain classification problem and achieved high performance. However, based on our observation, it incurs a class weight bias between old and new classes: the norm of weights of old classes is smaller than that of new classes and the gap continually widens as learning progresses. Denote the parameters in $g(\cdot)$ as $\mathbf{W} \in \mathbb{R}^{K \times d}$, where d is the dimension of feature $h(x)$ and K is the number of classes. k -th row vector in \mathbf{W} is denoted as \mathbf{w}_k , which is the weight vector corresponding to class k .

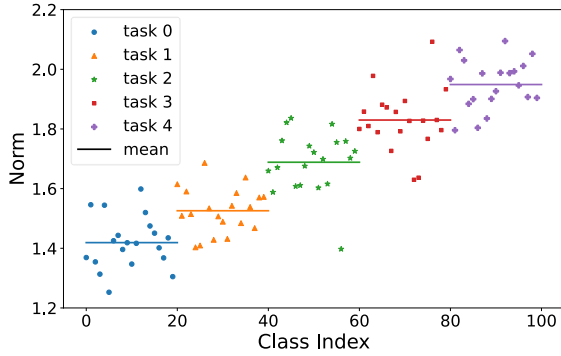


Fig. 3. The norms of class weights in the standard 5-task setting.

We plot the weight norm versus the class order of tasks in Figure 3. We analyze the underlying reasons and propose a simple solution to the problem below.

1) **Analysis of Weight Bias:** A direct reason behind the class weight bias is the data imbalance problem. A similar observation is reported in [17], where data imbalance is caused by limited data memory. Different from that, the inversion-based methods can generate arbitrarily balanced and enough training samples. However, it is not the first choice in practice for the reason of low generation efficiency and poor generation quality. As a replacement, a batch of real new samples and a batch of generated old samples are used for training every iteration. The batch size is fixed across tasks. This will inevitably cause a data imbalance problem. For synthetic samples, the past class samples become fewer in a batch when past classes become more. But for real samples, the number of samples in each class is stable. What is more, the bias will increase as the incremental learning process continues due to the accumulation effect.

However, when we control the number of classes of synthetic and real data to be the same, the weight bias problem still exists (as shown in Figure 4(a)). It indicates the existence of other reasons. We argue different loss functions and different training data may also contribute to weight bias and thus design a two-task class incremental experiment to uncover the factors concerned with it. The first task includes data from 50 classes of CIFAR-100 while the second task includes the other 50 classes. Training with standard CE is adopted for the first task. As for the second task, we compare 4 training schemes: (1) synthetic (HKD) - real (LCE), which is the standard training scheme, (2) real (LCE) - real (LCE), where real old data is used and trained with local CE loss, (3) real (HKD) - real (LCE), where the real old data is used, (4) synthetic (LCE) - real (LCE), where the synthetic old data is trained with the local CE loss. We report the norm of class weights at the end of task two.

First of all, Figure 4(b) shows an unbiased situation under the condition of equal losses and data quality for both tasks. Further, results in Figure 4(c) and 3(d) validate our hypothesis that both the different training losses and different properties of training data will have effects on the class weights. HKD loss calculates the mean square error (MAE) of the logits of the old and new models as defined in Equation (5). LCE loss defined

in Equation (6) is a cross-entropy loss applied locally among part of classes. To be noticed, MAE loss tends to oscillate near the optimal point while cross-entropy loss can always be minimized by larger class weight norms (*e.g.*, by scaling). Thus, it is natural to find the norms of new class weights with LCE loss are bigger than those of old class weights with HKD loss in Figure 4(c).

On the other hand, we attribute the bias caused by synthetic samples (as shown in Figure 4(d)) to their poor separability. Due to the limited generation quality, the synthetic sample tends to mix many features of different classes [13]. Thus it introduces noisy information when training the classifier $g(\cdot)$ and resultantly causes a large variance in the gradient direction of $g(\cdot)$ with different samples. Assume there are M batches within one epoch. At each batch B^m , the derivative of \mathcal{L}_{lce}^m with respect to \mathbf{w}_k is $\frac{\partial \mathcal{L}_{lce}^m}{\partial \mathbf{w}_k}$. The gradient direction variance is reflected in the ratio of the norm of the mean gradient vector to the mean norm of gradient vectors, denoted as R_k as follows:

$$R_k = \frac{\left\| \frac{1}{M} \sum_{m=1}^M \frac{\partial \mathcal{L}_{lce}^m}{\partial \mathbf{w}_k} \right\|}{\frac{1}{M} \sum_{m=1}^M \left\| \frac{\partial \mathcal{L}_{lce}^m}{\partial \mathbf{w}_k} \right\|} = \frac{\left\| \sum_{m=1}^M \frac{\partial \mathcal{L}_{lce}^m}{\partial \mathbf{w}_k} \right\|}{\sum_{m=1}^M \left\| \frac{\partial \mathcal{L}_{lce}^m}{\partial \mathbf{w}_k} \right\|} \leq 1. \quad (14)$$

If the direction variance is large, R_k tends to be small and vice versa. On top of that, we employ $\bar{R} = \frac{1}{|C|} \sum_{k \in C} R_k$ as the metric for measuring the variance regarding the norms of all class vectors. Notably, we split the dataset into batches to simulate the real scene during training. We plot \bar{R} of classes belonging to synthetic and real samples in the synthetic (LCE) - real (LCE) scheme as shown in Figure 5. It shows that the gradient direction variance of class weights of real data is smaller than that of synthetic data in the whole training stage. It is conducive to a fast convergence and stable promotion of the weight norm, which explains the phenomenon of Figure 4(d). The new observation about data quality suggests explicit debiasing strategy is preferred and debiasing methods [48], [52] focusing on split loss functions may not be compatible with synthetic data in DFCIL. Results of the comparison with different debiasing methods can be found in Section V-C.

2) **Weight Alignment Regularization Loss:** To correct the bias, we try to align the weights of old and new classes. Though a post-processing alignment strategy is provided in [17], it is not that suitable for data consistency enhancement and will still cause bias among tasks as shown in Section V-C. We prefer to replay data through an unbiased trained model to maximize the satisfaction of the Gaussian assumption. If we align the weights after training, the feature extractor will be biased and the tied covariance may be a biased estimation. So we regularize it during training. Denoting the norm of $\|\mathbf{w}_k\|_2$ as n_k , the mean norm of old and new class weights as n_{old}, n_{new} , the regularization is as follows:

$$\mathcal{L}_{war} = \frac{1}{|C_{0:i}|} \left(\sum_{k \notin C_i} |n_k - n_{new}| + \sum_{k \in C_i} |n_k - n_{old}| \right), \quad (15)$$

As a result, the overall loss for the training stage is:

$$\mathcal{L}_{train} = \mathcal{L}_{T_base} + \lambda_{war} \mathcal{L}_{war}. \quad (16)$$

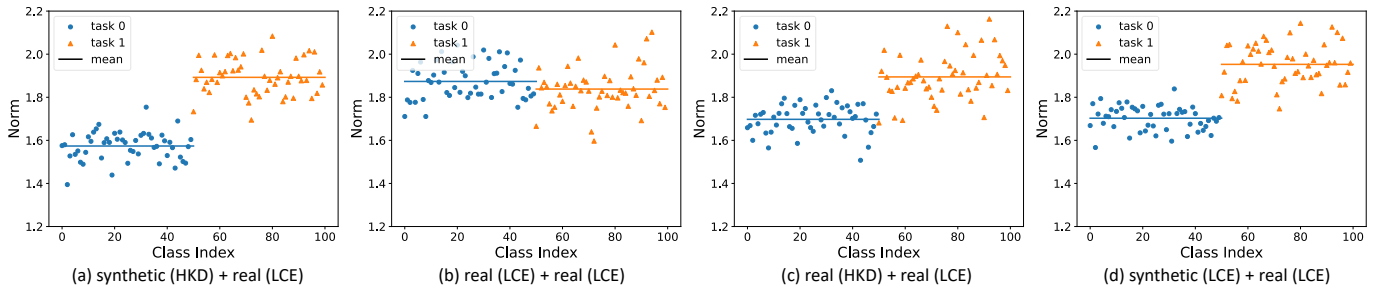


Fig. 4. The norms of class weights in 2-task experiments with different training schemes for the second task. (a) the standard training scheme. (b) a scheme where real old data is used and trained with local CE loss. (c) a scheme where the real old data is used. (d) a scheme where the synthetic old data is trained with the local CE loss. We report the results at the end of the final task.

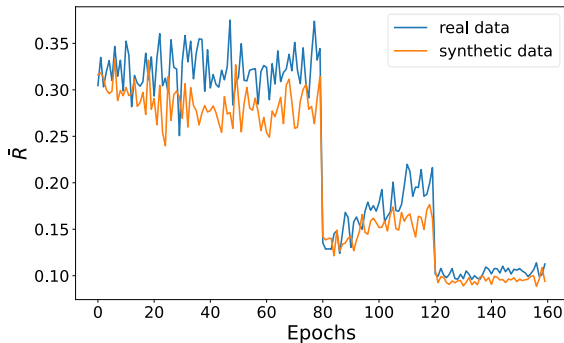


Fig. 5. \bar{R} of class weights belonging to synthetic and real data in the training process of task two in the synthetic (LCE) - real (LCE) scheme. \bar{R}_{real} is larger than $\bar{R}_{synthetic}$, which indicates a more stable gradient direction of class weights of real data.

V. EXPERIMENTS

In this section, we perform experiments to evaluate our proposed CCIL framework. First, we compare CCIL with other SOTA methods on several class incremental learning benchmarks to show its superiority. Then, we perform the ablation study on the key designs of our proposed CCIL framework and we also conduct parameter analysis experiments.

A. Experimental Settings

We compare the performance of methods on three vision classification benchmark datasets: CIFAR-100 [2], Tiny-ImageNet [53], ImageNet-100 [1]. All three datasets are composed of natural images but differ in the scales of the datasets and sizes of contained images. CIFAR-100 [2] consists of 60K images where each class has 500 images for the training and 100 images for the test. CIFAR-100 is a relatively small dataset and the image size of CIFAR-100 is 32×32 . Tiny-ImageNet [53] is a medium-sized dataset, which contains 100K images of 200 classes. The image size of Tiny-ImageNet is larger than that of CIFAR-100 and up to 64×64 . ImageNet [1] is a large visual dataset consisting of natural images in high resolution. We use the ImageNet-100 subset for efficiency, which has 100 classes and 1.3K training images and 50 validation images per class. The three datasets cover images from different sizes and all have enough classes and samples per class for incremental learning. Specifically, we

follow prior works [12], [13] to equally split the classes into 5, 10, and 20 tasks and learn from them continually.

To measure the performance, we adopt the last incremental accuracy A_N and the mean incremental accuracy \bar{A} as metrics. A_N denotes the classification accuracy on all seen classes after learning the last task. $\bar{A} = \sum_{i=1}^N A_i$ averages the results of different learning phases and measures the performance of the model through the whole training. Formally, A_i is defined as follows:

$$A_i = \frac{1}{|X_{test}^{0:i-1}|} \sum_{(x,y) \in X_{test}^{0:i-1}} \mathbb{I}(\operatorname{argmax}_k f_{0:i-1}(x)_k = y), \quad (17)$$

where $\mathbb{I}(\cdot)$ is the indicator function.

The basic training settings of CCIL are kept the same as baselines for fair comparison [12], [13]. Specifically, the backbone network for CIFAR-100 and Tiny-ImageNet is a 32-layer ResNet [3]. And for ImageNet-100, we adopt Resnet18 [3] as the backbone. At each task of CIFAR-100 or Tiny-ImageNet, we train the model for 200 epochs. The learning rate is set at 0.1 initially and decayed by 10 at epoch 80 and 120. The weight decay is 0.0005 for CIFAR-100 and 0.0002 for Tiny-ImageNet. We use SGD optimizer and the batch size is set as 128. For ImageNet-100, we train the model for 120 epochs. The learning rate is 0.1 and decayed at epoch 30 and 60 and the weight decay is set as 0.0001. We use SGD optimizer and the batch size is set as 64. For the generation, we use different generative models for different datasets to generate images of the same size as the real ones. We use the Adam optimizer with a constant learning rate 0.001. We train the generative model for 5000 steps when synthesizing images of CIFAR and Tiny-ImageNet and we train for 10000 steps when synthesizing images of ImageNet.

We perform CIFAR-100 and Tiny-ImageNet experiments on an RTX 2080Ti GPU while we perform ImageNet-100 experiments on an V100 GPU. For CIFAR-100 and Tiny-ImageNet experiments, we report the mean \pm std% results based on 3 different class orders. For ImageNet-100 experiments, we report the result based on the same class order. The class orders are set as the same in [13].

B. Incremental Learning Performance

To validate the effectiveness of the proposed CCIL method, we compare it with several baselines. We briefly introduce

TABLE II

PERFORMANCE ON CIFAR-100. THE DATASET IS DIVIDED INTO 5, 10 AND 20 TASKS. * INDICATES THE RESULTS REPORTED IN [13].

Method	5		10		20	
	A_N	\bar{A}	A_N	\bar{A}	A_N	\bar{A}
DGR*	14.40 ± 0.40	-	8.10 ± 0.10	-	4.10 ± 0.30	-
LwF*	17.00 ± 0.10	-	9.20 ± 0.00	-	4.70 ± 0.10	-
DeepInversion*	18.80 ± 0.30	-	10.90 ± 0.60	-	5.70 ± 0.30	-
ABD	46.79 ± 0.21	63.16 ± 1.58	37.01 ± 1.46	57.32 ± 2.32	22.14 ± 0.63	44.53 ± 1.62
R-DFCIL*	50.47 ± 0.43	64.85 ± 1.78	42.37 ± 0.72	59.41 ± 1.76	30.75 ± 0.12	48.47 ± 1.90
R-DFCIL	49.90 ± 0.23	64.78 ± 2.23	42.57 ± 0.71	59.13 ± 1.70	30.35 ± 0.12	47.80 ± 1.81
CCIL(ABD)	50.27 ± 0.51	64.89 ± 1.24	40.01 ± 0.86	58.86 ± 2.00	25.46 ± 0.40	46.85 ± 1.43
CCIL(R-DFCIL)	52.46 ± 0.35	66.31 ± 1.46	43.69 ± 0.57	60.14 ± 1.87	31.72 ± 0.22	49.01 ± 1.81

TABLE III

PERFORMANCE ON TINY-IMAGENET. THE DATASET IS DIVIDED INTO 5, 10 AND 20 TASKS. * INDICATES THE RESULTS REPORTED IN [13].

Method	5		10		20	
	A_N	\bar{A}	A_N	\bar{A}	A_N	\bar{A}
ABD	30.40 ± 0.78	45.07 ± 0.78	22.50 ± 0.62	40.52 ± 0.71	15.65 ± 0.95	35.00 ± 0.53
R-DFCIL*	35.89 ± 0.75	48.96 ± 0.40	29.58 ± 0.51	44.36 ± 0.18	24.43 ± 0.82	39.34 ± 0.18
R-DFCIL	35.25 ± 0.57	48.90 ± 1.03	29.96 ± 0.36	44.58 ± 0.68	24.07 ± 0.28	39.06 ± 0.62
CCIL(ABD)	33.04 ± 0.30	46.95 ± 0.73	25.45 ± 0.48	42.56 ± 1.05	16.92 ± 0.56	36.09 ± 0.63
CCIL(R-DFCIL)	36.89 ± 0.73	49.69 ± 0.76	30.90 ± 0.52	45.29 ± 0.73	24.54 ± 0.27	39.65 ± 0.19

TABLE IV

PERFORMANCE ON IMAGENET-100. THE DATASET IS DIVIDED INTO 5, 10 AND 20 TASKS. * INDICATES THE RESULTS REPORTED IN [13].

Method	5		10		20	
	A_N	\bar{A}	A_N	\bar{A}	A_N	\bar{A}
ABD	52.04	67.00	38.34	58.08	21.74	44.69
R-DFCIL*	53.10	68.15	42.28	59.10	30.28	47.33
R-DFCIL	50.90	67.72	41.38	58.82	27.86	45.74
CCIL(ABD)	56.02	69.42	41.86	60.52	25.88	48.10
CCIL(R-DFCIL)	56.80	70.39	46.04	62.66	34.60	49.18

TABLE V

COMPARISONS WITH OTHER DEBIASING METHODS ON CIFAR-100. ALL NUMBERS IN THE TABLE ARE LAST INCREMENTAL ACCURACY (MEAN ± STD%).

Method	5	10	20
SCE	47.86 ± 0.51	36.00 ± 0.55	22.43 ± 0.76
ACE	47.11 ± 0.32	35.13 ± 0.91	21.75 ± 0.83
SSIL	51.52 ± 0.31	42.81 ± 0.90	28.96 ± 0.11
WA	51.08 ± 0.58	42.41 ± 0.59	29.81 ± 0.32
CCIL	52.46 ± 0.35	43.69 ± 0.57	31.72 ± 0.22

them as follows:

Deep Generative Replay [10] (DGR): a generative data replay method, which needs to keep a generative model all the time during the whole incremental learning process.

Learning without Forgetting [36] (LwF): a classic data-free class incremental method.

DeepInversion [14]: a data-free data replay-based class incremental method, which replays data by model inversion without saving a generative model.

Always Be Dreaming [12] (ABD): a strong baseline, which keeps the inversion stage almost the same as [14] and changes the training stage for better performance.

Relation-Guided Representation Learning [13] (R-DFCIL): the SOTA baseline, which keeps the inversion stage the same as [12] and further ameliorates the training stage.

Because CCIL focuses on the inversion stage and the regularization of the classifier, which is orthogonal to SOTA works, we combine it with them (R-DFCIL and ABD) for evaluation. To make a fair comparison, we keep the specific training settings of CCIL the same as the combined baseline. If not explicitly mentioned, CCIL refers to CCIL + R-DFCIL in the following. We report the results of CIFAR-100 in Table II, the results of Tiny-ImageNet in Table III, and the results of ImageNet-100 in Table IV. From all three tables, we can see that our CCIL method can achieve consistent improvements

both in A_N and \bar{A} compared to the baselines. Specifically, CCIL surpasses the second-best method by 2.5, 1.1, and 1.4 percent in A_N on CIFAR-100. Likely, the absolute gains are 1.6, 0.9, and 0.5 on Tiny-ImageNet, and the improvements achieve 5.9, 4.7, and 6.7 on ImageNet-100. What is more, we can see that both R-DFCIL and ABD can benefit from the CCIL framework consistently, which verifies the applicability of CCIL. In addition, the results in \bar{A} are consistent with results in A_N , which indicates that CCIL can improve performance in the whole learning process.

C. Comparisons with Other Debiasing Approaches

In Section IV-C, we identify two reasons for class weight bias encountered in the inversion-based incremental learning process and propose a simple regularization term L_{war} to align the weights. In this section, we compare the proposed strategy with some known approaches in the literature that can help reduce bias. We will briefly describe these approaches as follows:

Split Cross Entropy (SCE): SCE applies two independent local CE losses (see Equation (6)) on the replay data and the data from the new task. Local means the Softmax is calculated locally on old classes or new classes.

Asymmetric Cross Entropy [48] (ACE): ACE applies the local CE loss on the data from the new task and applies the

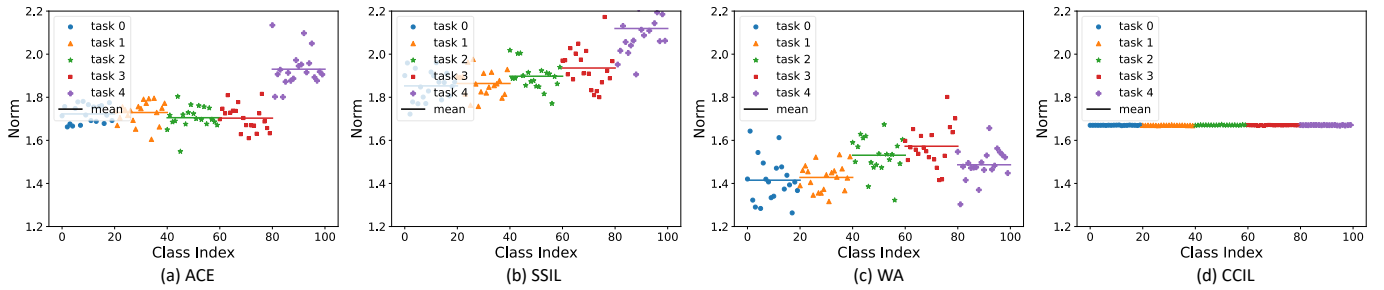


Fig. 6. The norms of class weights in 5-task experiments with different debiasing approaches. (a) Asymmetric Cross-entropy. (b) Separated-Softmax for Incremental Learning. (c) Weight Aligning. (d) CCIL with Weight Alignment Regularization.

global CE loss on the replay data, which further impedes the improvement of the norms of new classes.

Separated-Softmax for Incremental Learning [52] (SSIL): On top of SCE, SSIL adopts task-wise KD loss to preserve knowledge within each task to avoid bias among tasks.

Weight Aligning [17] (WA): WA is a post-processing alignment method. After training the model, WA aligns the mean norm of old and new classes by multiplying the weight vectors of new classes by a scalar.

The approaches above can be divided into two classes: (1) split losses for data of old and new classes or even for data of each task (SCE, ACE, and SSIL), (2) explicit post-processing class weight alignment (WA). For the first line of approaches, we keep the inversion stage the same as CCIL and replace L_{hkd} with the proposed losses for fair comparisons. For WA, we keep both the inversion and the training stage the same as CCIL and align the weight after the training stage.

We compare these methods by both the weight alignment situation and the final classification performance. The experiments are carried out on the CIFAR-100 dataset and the classification performance is reported in Table V. In addition, we observe the weight alignment situation at the end of the last task in the 5-task setting, as shown in Figure 6. Note that SCE performs similarly to ACE and the 2-task situation of SCE can be obtained by referring to Figure 4(d).

From the results, we can see that SCE and ACE can mitigate the weight bias among old classes but can not mitigate the bias between new and old classes due to the data reason detailed in Section IV-C. What is more, lacking information on non-target classes is attributed to the large drop in performance. SSIL intends to separate classes by tasks and keep information on non-target classes when distillation. Thus, though existing bias like SCE, it would not affect the performance much. As for WA, it performs the debiasing between old and new classes but lacks constraint within old classes, where the bias can be observed. What is more, the way of post-processing can not guarantee debiasing in the training stage which can result in a biased feature extractor and hurt the data consistency enhancement by contradicting the assumption. These factors incur the suboptimal performance of WA. Different from them, our CCIL avoids these disadvantages and mitigates the bias explicitly. However, CCIL does not keep the relative magnitude of the norms of the weight vectors within the

TABLE VI
ABLATION STUDY. WE ABLATE EACH COMPONENT OF CCIL. ALL NUMBERS IN THE TABLE ARE LAST INCREMENTAL ACCURACY (MEAN \pm STD%).

Method	5	10	20
R-DFCIL	49.90 \pm 0.23	42.57 \pm 0.71	30.35 \pm 0.12
CCIL–DCE	50.95 \pm 0.18	42.96 \pm 0.98	31.08 \pm 0.32
CCIL–WAR	50.86 \pm 0.34	43.52 \pm 0.99	31.27 \pm 0.19
CCIL	52.46 \pm 0.35	43.69 \pm 0.57	31.72 \pm 0.22

task. We guess that task-wise alignment rather than class-wise alignment in CCIL is enough to mitigate the bias, which we will leave for future work.

D. Ablation Study

The two main contributions of CCIL are the proposed data consistency-enhanced (DCE) loss and the weight alignment regularization (WAR) loss. The DCE loss is applied in the inversion stage and the WAR loss is used in the training stage. To validate the effectiveness of every component of the proposed CCIL, we ablate DCE and WAR respectively. As a result, we have 4 combinations: (1) CCIL. The complete framework with both loss terms, (2) CCIL–WAR. CCIL framework without the WAR loss in the training stage, (3) CCIL–DCE. CCIL framework without DCE loss in the inversion stage, (4) R-DFCIL. CCIL degrades to R-DFCIL without both DCE and WAR loss. We conduct experiments on CIFAR-100 as shown in Table VI.

Results suggest that each component can help improve the final incremental accuracy in all settings with different numbers of tasks. To be noticed, the DCE component has a more significant effect on the final performance compared to the WAR component. Further combining them achieves the best results.

E. Parameter Analysis

In the CCIL framework, we keep the hyperparameters the same as them in [13] and there left two new hyperparameters λ_{dce} and λ_{war} to tune. We conduct the parameter analysis on CIFAR-100 with 5, 10, and 20 tasks. Because λ_{dce} and λ_{war} are introduced in the different stages, we perform two separate searches. First, we fix $\lambda_{war} = 0.1$ and search the optimal λ_{dce} . We tried $\lambda_{dce} = 0.01, 0.02, 0.05, 0.1, 0.2$. As shown in the left subfigure of Figure 7, the last incremental

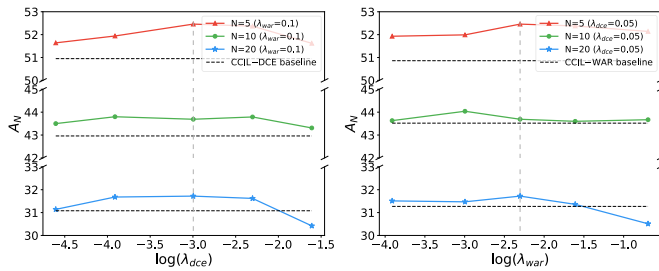


Fig. 7. The influence of λ_{dce} and λ_{war} on CIFAR-100 with 5, 10 and 20 tasks. Left, search λ_{dce} when λ_{war} is fixed. Right, search λ_{war} when λ_{dce} is fixed.

accuracy first increases and then decreases as λ_{dce} increases, which indicates that a local optimum exists. To be noticed, CCIL performs better than the corresponding baseline in most cases. Then we fixed $\lambda_{dce} = 0.05$ and search λ_{war} in the range of $\{0.02, 0.05, 0.1, 0.2, 0.5\}$. Results in Figure 7 demonstrate that the performance is relatively less sensitive to λ_{war} than λ_{dce} . The performance gain is close except when the regulation strength is set too high and the number of tasks is 20. Similarly, a wide range of values of λ_{war} has positive effects on the final performance. According to the results, we set $\lambda_{dce} = 0.05$, $\lambda_{war} = 0.1$ to fit CIFAR-100 with different numbers of tasks and further adopt them in Tiny-ImageNet and ImageNet-100 experiments. More surprisingly, we also adopt the same parameters in the CCIL + ABD experiments and it works well. Results in Section V-B validate the good transferability of the parameters.

VI. CONCLUSION

In this paper, we propose CCIL framework to solve the catastrophic forgetting problem in data-free incremental learning. To address the data inconsistency problem in the literature, we first propose quantitative measures of data consistency. With them, we further analyze existing losses, which gives several insights and inspires the development of a novel loss term. Specifically, by aligning the statistical parameters in the feature space, we narrow the gap between synthetic and real data and ameliorate the inversion stage. This approach proves to be easy to implement. Furthermore, we identify a phenomenon where the norms of old class weights decrease as learning progresses. We analyze the underlying reasons in the background of DFCIL and propose a simple and effective regularization term to reduce the weight bias. Experiments on different datasets show our method can surpass previous works and achieve SOTA performance. Also importantly, we believe the comprehensive analysis of multiple aspects of data-free data replay methods in our study will contribute to the ongoing efforts in developing more effective techniques.

REFERENCES

- [1] J. Deng, W. Dong, R. Socher, L.-J. Li, K. Li, and L. Fei-Fei, "Imagenet: A large-scale hierarchical image database," in *2009 IEEE conference on computer vision and pattern recognition*. Ieee, 2009, pp. 248–255.
- [2] A. Krizhevsky, "Learning multiple layers of features from tiny images," University of Toronto, Toronto, ON, Canada, Tech. Rep., 2009.

- [3] K. He, X. Zhang, S. Ren, and J. Sun, "Deep residual learning for image recognition," in *Proceedings of the IEEE conference on computer vision and pattern recognition*, 2016, pp. 770–778.
- [4] X. Zhang, S. Dong, J. Chen, Q. Tian, Y. Gong, and X. Hong, "Deep class-incremental learning from decentralized data," *IEEE Transactions on Neural Networks and Learning Systems*, 2022.
- [5] M. McCloskey and N. J. Cohen, "Catastrophic interference in connectionist networks: The sequential learning problem," in *Psychology of learning and motivation*. Elsevier, 1989, vol. 24, pp. 109–165.
- [6] S.-A. Rebuffi, A. Kolesnikov, G. Sperl, and C. H. Lampert, "icarl: Incremental classifier and representation learning," in *Proceedings of the IEEE conference on Computer Vision and Pattern Recognition*, 2017, pp. 2001–2010.
- [7] A. Douillard, M. Cord, C. Ollion, T. Robert, and E. Valle, "Podnet: Pooled outputs distillation for small-tasks incremental learning," in *European Conference on Computer Vision*. Springer, 2020, pp. 86–102.
- [8] H. Zhao, H. Wang, Y. Fu, F. Wu, and X. Li, "Memory-efficient class-incremental learning for image classification," *IEEE Transactions on Neural Networks and Learning Systems*, vol. 33, no. 10, pp. 5966–5977, 2021.
- [9] N. Kamra, U. Gupta, and Y. Liu, "Deep generative dual memory network for continual learning," *arXiv preprint arXiv:1710.10368*, 2017.
- [10] H. Shin, J. K. Lee, J. Kim, and J. Kim, "Continual learning with deep generative replay," *Advances in neural information processing systems*, vol. 30, 2017.
- [11] M. Zhai, L. Chen, F. Tung, J. He, M. Nawhal, and G. Mori, "Lifelong gan: Continual learning for conditional image generation," in *Proceedings of the IEEE/CVF International Conference on Computer Vision*, 2019, pp. 2759–2768.
- [12] J. Smith, Y.-C. Hsu, J. Balloch, Y. Shen, H. Jin, and Z. Kira, "Always be dreaming: A new approach for data-free class-incremental learning," in *Proceedings of the IEEE/CVF International Conference on Computer Vision*, 2021, pp. 9374–9384.
- [13] Q. Gao, C. Zhao, B. Ghanem, and J. Zhang, "R-dfcil: Relation-guided representation learning for data-free class incremental learning," *arXiv preprint arXiv:2203.13104*, 2022.
- [14] H. Yin, P. Molchanov, J. M. Alvarez, Z. Li, A. Mallya, D. Hoiem, N. K. Jha, and J. Kautz, "Dreaming to distill: Data-free knowledge transfer via deepinversion," in *Proceedings of the IEEE/CVF Conference on Computer Vision and Pattern Recognition*, 2020, pp. 8715–8724.
- [15] G. K. Nayak, K. R. Mopuri, V. Shaj, V. B. Radhakrishnan, and A. Chakraborty, "Zero-shot knowledge distillation in deep networks," in *International Conference on Machine Learning*. PMLR, 2019, pp. 4743–4751.
- [16] G. Fang, K. Mo, X. Wang, J. Song, S. Bei, H. Zhang, and M. Song, "Up to 100x faster data-free knowledge distillation," in *Proceedings of the AAAI Conference on Artificial Intelligence*, vol. 36, no. 6, 2022, pp. 6597–6604.
- [17] B. Zhao, X. Xiao, G. Gan, B. Zhang, and S.-T. Xia, "Maintaining discrimination and fairness in class incremental learning," in *Proceedings of the IEEE/CVF Conference on Computer Vision and Pattern Recognition*, 2020, pp. 13 208–13 217.
- [18] S. Yan, J. Xie, and X. He, "Der: Dynamically expandable representation for class incremental learning," in *Proceedings of the IEEE/CVF Conference on Computer Vision and Pattern Recognition*, 2021, pp. 3014–3023.
- [19] Z. Wu, C. Baek, C. You, and Y. Ma, "Incremental learning via rate reduction," in *Proceedings of the IEEE/CVF Conference on Computer Vision and Pattern Recognition*, 2021, pp. 1125–1133.
- [20] T.-Y. Wu, G. Swaminathan, Z. Li, A. Ravichandran, N. Vasconcelos, R. Bhotika, and S. Soatto, "Class-incremental learning with strong pre-trained models," in *Proceedings of the IEEE/CVF Conference on Computer Vision and Pattern Recognition*, 2022, pp. 9601–9610.
- [21] A. Douillard, A. Ramé, G. Couairon, and M. Cord, "Dytox: Transformers for continual learning with dynamic token expansion," in *Proceedings of the IEEE/CVF Conference on Computer Vision and Pattern Recognition*, 2022, pp. 9285–9295.
- [22] S. Lee, J. Ha, D. Zhang, and G. Kim, "A neural dirichlet process mixture model for task-free continual learning," *arXiv preprint arXiv:2001.00689*, 2020.
- [23] D. Maltoni and V. Lomonaco, "Continuous learning in single-incremental-task scenarios," *Neural Networks*, vol. 116, pp. 56–73, 2019.
- [24] M. Hersche, G. Karunaratne, G. Cherubini, L. Benini, A. Sebastian, and A. Rahimi, "Constrained few-shot class-incremental learning," in *Proceedings of the IEEE/CVF Conference on Computer Vision and Pattern Recognition*, 2022, pp. 9057–9067.

- [25] G. Shi, J. Chen, W. Zhang, L.-M. Zhan, and X.-M. Wu, "Overcoming catastrophic forgetting in incremental few-shot learning by finding flat minima," *Advances in Neural Information Processing Systems*, vol. 34, pp. 6747–6761, 2021.
- [26] A. F. Akyürek, E. Akyürek, D. Wijaya, and J. Andreas, "Subspace regularizers for few-shot class incremental learning," *arXiv preprint arXiv:2110.07059*, 2021.
- [27] S. Ebrahimi, M. Elhoseiny, T. Darrell, and M. Rohrbach, "Uncertainty-guided continual learning with bayesian neural networks," *arXiv preprint arXiv:1906.02425*, 2019.
- [28] Y.-M. Tang, Y.-X. Peng, and W.-S. Zheng, "Learning to imagine: Diversify memory for incremental learning using unlabeled data," in *Proceedings of the IEEE/CVF Conference on Computer Vision and Pattern Recognition*, 2022, pp. 9549–9558.
- [29] K. Lee, K. Lee, J. Shin, and H. Lee, "Overcoming catastrophic forgetting with unlabeled data in the wild," in *Proceedings of the IEEE/CVF International Conference on Computer Vision*, 2019, pp. 312–321.
- [30] A. K. Bhunia, V. R. Gajjala, S. Koley, R. Kundu, A. Sain, T. Xiang, and Y.-Z. Song, "Doodle it yourself: Class incremental learning by drawing a few sketches," in *Proceedings of the IEEE/CVF Conference on Computer Vision and Pattern Recognition*, 2022, pp. 2293–2302.
- [31] F. M. Castro, M. J. Marín-Jiménez, N. Guil, C. Schmid, and K. Alahari, "End-to-end incremental learning," in *Proceedings of the European conference on computer vision (ECCV)*, 2018, pp. 233–248.
- [32] X. Hu, K. Tang, C. Miao, X.-S. Hua, and H. Zhang, "Distilling causal effect of data in class-incremental learning," in *Proceedings of the IEEE/CVF Conference on Computer Vision and Pattern Recognition*, 2021, pp. 3957–3966.
- [33] S. Hou, X. Pan, C. C. Loy, Z. Wang, and D. Lin, "Learning a unified classifier incrementally via rebalancing," in *Proceedings of the IEEE/CVF Conference on Computer Vision and Pattern Recognition*, 2019, pp. 831–839.
- [34] Y. Liu, X. Hong, X. Tao, S. Dong, J. Shi, and Y. Gong, "Model behavior preserving for class-incremental learning," *IEEE Transactions on Neural Networks and Learning Systems*, 2022.
- [35] G. Hinton, O. Vinyals, J. Dean *et al.*, "Distilling the knowledge in a neural network," *arXiv preprint arXiv:1503.02531*, vol. 2, no. 7, 2015.
- [36] Z. Li and D. Hoiem, "Learning without forgetting," *IEEE transactions on pattern analysis and machine intelligence*, vol. 40, no. 12, pp. 2935–2947, 2017.
- [37] K. Zhu, W. Zhai, Y. Cao, J. Luo, and Z.-J. Zha, "Self-sustaining representation expansion for non-exemplar class-incremental learning," in *Proceedings of the IEEE/CVF Conference on Computer Vision and Pattern Recognition*, 2022, pp. 9296–9305.
- [38] M. PourKeshavarzi, G. Zhao, and M. Sabokrou, "Looking back on learned experiences for class/task incremental learning," in *International Conference on Learning Representations*, 2021.
- [39] I. Goodfellow, J. Pouget-Abadie, M. Mirza, B. Xu, D. Warde-Farley, S. Ozair, A. Courville, and Y. Bengio, "Generative adversarial networks," *Communications of the ACM*, vol. 63, no. 11, pp. 139–144, 2020.
- [40] K. Muandet, D. Balduzzi, and B. Schölkopf, "Domain generalization via invariant feature representation," in *International Conference on Machine Learning*. PMLR, 2013, pp. 10–18.
- [41] S. Motiian, M. Piccirilli, D. A. Adjeroh, and G. Doretto, "Unified deep supervised domain adaptation and generalization," in *Proceedings of the IEEE international conference on computer vision*, 2017, pp. 5715–5725.
- [42] H. Li, S. J. Pan, S. Wang, and A. C. Kot, "Domain generalization with adversarial feature learning," in *Proceedings of the IEEE conference on computer vision and pattern recognition*, 2018, pp. 5400–5409.
- [43] K. Lee, K. Lee, H. Lee, and J. Shin, "A simple unified framework for detecting out-of-distribution samples and adversarial attacks," *Advances in neural information processing systems*, vol. 31, 2018.
- [44] P. Morteza and Y. Li, "Provable guarantees for understanding out-of-distribution detection," in *Proceedings of the AAAI Conference on Artificial Intelligence*, vol. 8, 2022.
- [45] W. Liu, X. Wang, J. Owens, and Y. Li, "Energy-based out-of-distribution detection," *Advances in Neural Information Processing Systems*, vol. 33, pp. 21 464–21 475, 2020.
- [46] Y. Sun, C. Guo, and Y. Li, "React: Out-of-distribution detection with rectified activations," *Advances in Neural Information Processing Systems*, vol. 34, pp. 144–157, 2021.
- [47] K. Joseph, S. Khan, F. S. Khan, R. M. Anwer, and V. N. Balasubramanian, "Energy-based latent aligner for incremental learning," in *Proceedings of the IEEE/CVF Conference on Computer Vision and Pattern Recognition*, 2022, pp. 7452–7461.
- [48] L. Caccia, R. Aljundi, N. Asadi, T. Tuytelaars, J. Pineau, and E. Belilovsky, "New insights on reducing abrupt representation change in online continual learning," *arXiv preprint arXiv:2203.03798*, 2022.
- [49] X. Zhou, X. Liu, D. Zhai, J. Jiang, X. Gao, and X. Ji, "Learning towards the largest margins," *arXiv preprint arXiv:2206.11589*, 2022.
- [50] D. W. Scott, *Multivariate density estimation: theory, practice, and visualization*. John Wiley & Sons, 2015.
- [51] D. Hendrycks and K. Gimpel, "A baseline for detecting misclassified and out-of-distribution examples in neural networks," *arXiv preprint arXiv:1610.02136*, 2016.
- [52] H. Ahn, J. Kwak, S. Lim, H. Bang, H. Kim, and T. Moon, "Ssil: Separated softmax for incremental learning," in *Proceedings of the IEEE/CVF International conference on computer vision*, 2021, pp. 844–853.
- [53] Y. Le and X. Yang, "Tiny imagenet visual recognition challenge," *CS 231N*, vol. 7, no. 7, p. 3, 2015.